MASTER

UCID- 18250

Lawrence Livermore Laboratory

A FINITE ELEMENT ANALYSIS OF STEMMING LOADS ON PIPES

Dennis E. Maiden

August 1979

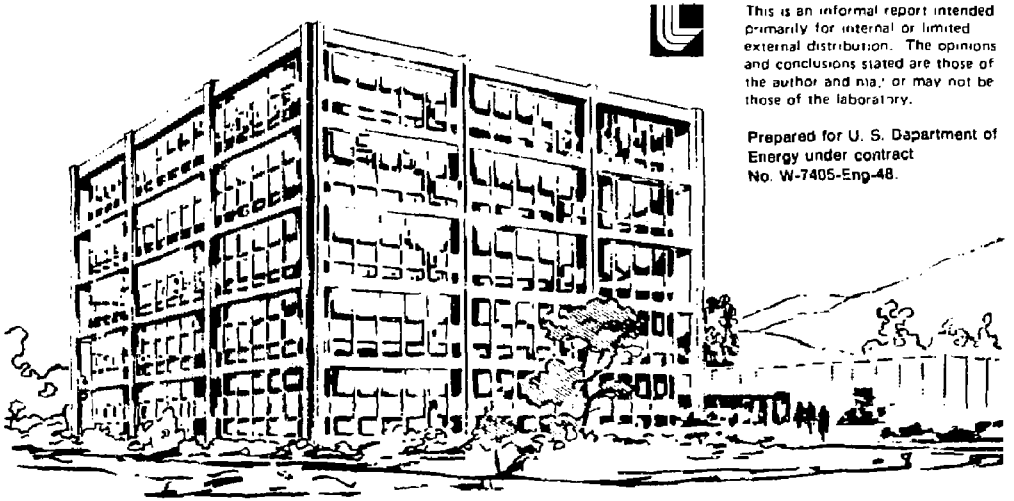

Prepared for U. S. Department of Energy under contract No. W-7405-Eng-48.

A Finite Element Analysis of Stemming Loads on Pipes

Dennis E. Maiden

Lawrence Livermore Laboratory, University of California
Livermore, California 94550

ABSTRACT

A computational model has been developed for calculating the loads and displacements on a pipe placed in a hole which is subsequently filled with soil. A composite soil-pipe finite element model which employs fundamental material constants in its formalism is derived. The shear modulus of the soil, and the coefficient of friction at the pipe are the important constants to be specified. The calculated loads on the pipe are in agreement with experimental data for layered and unlayered stemming designs. As a result more economical designs of the pipe string can be realized.

1.0 Introduction

Nuclear experiments are placed in holes up to 3000 feet deep and 8 feet in diameter and are supported from the surface by a pipe that is typically 9-5/8 inch in diameter. The holes are stemmed (filled) with layers of sand, gravel, fines, and shielding materials and at various depths asphalt plugs are placed to further insure no radioactive leakage. The pipe, therefore, must be designed to carry its own weight plus the weight induced by the stemming which may be for unlayered schemes 1 to 1.5 times the weight of the pipe. Typical configurations are shown in Figs. 1 and 2.

There are three mechanisms which contribute to the load on the pipe. The first is the load acting on the projected area of the device-diagnostic canister which is significant when magnetite is used. The second is the weight of the stemming material that is distributed between the pipe and the hole wall in proportion to their parimeters (the "wetted perimeter method"). The third is load relaxation due to the elasticity of the pipe and the soil which causes the pipe load to be transferred to the hole wall by shear.

An early method of calculating loads on the pipe string is due to Hamilton.[1] He used the wetted perimeter method but the predicted loads were too large by a factor of 3. Norris[2] accounted for this discrepancy by modeling the pipe as an elastic rod on an elastic foundation. Initially the pipe is held rigid until the hole is filled. The pipe is then allowed to relax causing part of the pipe load to be transferred to the hole wall in proportion to the soil spring stiffness. Unfortunately his stiffness was arbitrary and did not depend on the shear modulus of the soil or the geometry of the hole.

Staats[3] in collaboration with Norris and Kleck wrote a finite element code, STEM, to model the stemming operation by accounting for the deflection of the pipe as the stemming rises. The pipe, shown in Fig. 2, is divided into 1 foot elastic pipe elements. The filling process is modeled by applying the wetted perimeter load at 1 foot increments. At each increment a soil shear spring, which is proportional to the pipe displacement, is switched on, and the load and displacements calculated. This process is repeated for each increment using as initial conditions the loads and displacements from the previous increment. Pipe slippage is modeled by permitting only a maximum shear stress, Tau, to exist at the pipe wall. The STEM code, however, requires the following 6 constants:

1. K_s is the soil spring constant. In order to make the spring constant sensitive to hole geometry we multiply K_s by $\frac{D_p}{D_p+Alpha*D_h}$ where D_p is the pipe diameter and D_h the hole diameter.
2. Alpha - Geometry factor accounting for hole geometry.
3. Tau - Allowable shear stress at the pipe to allow slippage.
4. KBC - Soil spring constant on bottom of canister, drag plates, plastic plugs, and backfill bridges.
5. DIAMS - Soil support springs are turned on when backfill surface is DIAMS = (hole dia - WP dia)/2 where WP dia = cables + pipe diameter.
6. HT2D - Used to calculate the concentrated backfill load, $P = \gamma_s * \pi * R_p^2 * HT2D * 2 * R_p$, above canisters.

The most significant constants are K_s and Tau which are not material properties and are obtained from normalizing the code to predict conservative results.

Despite the many good ideas inherent in the STEM code it has a number of limitations, some of which have been pointed out by Blake.[5] The main limitation is that K_s should depend explicitly on the shear modulus and Tau on the coefficient of pipe friction and both on the local geometry. Furthermore Staats[4] suggests that Tau option in STEM may not be properly implemented. In addition, the constants employed in STEM were normalizing with past test results and are no longer valid for the new layered (pea gravel, LLL mix) scheme.

For these reasons an improved set of equations were derived and a new finite element code STMLOD was written. The new code contains the basic ideas of the STEM code, i.e., accounting for the deflection of the pipe as the stemming rises and local pipe slip when the shear at the pipe reaches a specified value. In addition, a new differential equation was added that relates the deflection of the pipe to the shear deformation of the soil. As a result, the load transfer between the pipe and the soil is described explicitly in terms of the shear modulus of the soil G_s and the coefficient of friction of the pipe μ_p as well as the geometry of the hole.

In this report Section 2 presents the mathematical model of the stemming process. Section 3 describes the numerical finite element method used to solve the equations. Section 4 discusses the material constants employed in the computations and their comparison with experimental data. Section 5 contains a presentation of results for layered and unlayered stemming schemes and a comparison with experimental data. The effects of pipe slip and thermal stresses are also presented.

The new set of equations described here was first presented at a seminar given by me on July 13, 1977 and attended by A. Blake, R. Corallo, S. Cowin, and F. Morrison. A users manual[6] for STMLOD was published in August, 1977 which contained results for the unlayered LLL-mix stemming scheme (Fig. 8). In this scheme, pipe slip was not important but the option was available. The new results presented here are for the layered LLL-mix, pea gravel scheme (Fig. 2) where pipe slip and thermal stresses are emphasized.

2.0 Mathematical Model

The governing equations for the pipe-soil interaction problem are the "bin theory" equations and can be derived from Fig. 4.

2.1 Differential Equations

a. Pipe force balance

$$\frac{dP}{dx} + \pi\gamma_s(R_H^2 - R_p^2) - 2\pi R_H\tau_H - \pi(R_H^2 - R_p^2)\frac{d\sigma}{dx} + \gamma_p - A_pE\alpha(T-T_o) = 0 \qquad (1)$$

where P is the pipe load, γ_s the soil weight density, R_H the hole radius, R_p the pipe radius, τ_H the shear stress at the hole wall, σ the vertical stress in the soil, γ_p is the weight per unit length of the pipe, α is the coefficient of thermal expansion, T is the temperature, and T_o the initial temperature.

b. Pipe deflection

$$\frac{dU}{dx} = \frac{P}{A_pE} \qquad (2)$$

where U is the pipe deflection, A_p the pipe area, and E the modulus of elasticity of the pipe.

c. Soil deflection

$$\frac{dU_s}{dr} = \frac{\tau}{G_s} \tag{3}$$

where U_s is the soil deflection, τ the shear stress in the soil, and G_s the shear modulus of the soil.

d. Soil force balance

$$2\pi r\tau = -2\pi R_H \tau_H + \pi \gamma_s (R_H^2 - r^2) - \pi (R_H^2 - r^2) \frac{d\sigma}{dx} \tag{4}$$

The γ_p term in Eq. (1) can be dropped by calculating the initial weight of the pipe directly, i.e.

$$P = \gamma_p (L_0 - x) \tag{5}$$

where γ_p is the pipe weight per unit length, L_0 is the length of the pipe, and x is measured from the top of the pipe. The thermal stress term in Eq. (1) can be included separately and will be discussed in detail in Sec. 3. The $\frac{d\sigma}{dx}$ term in Eqs. 1 and 4 is small and can be neglected for reasons given in the Appendix. Eqs. 1 to 4 become

a. Pipe force balance

$$\frac{dP}{dx} + \gamma_s \pi (R_H^2 - R_p^2) - 2\pi R_H \tau_H = 0 \tag{6}$$

b. Pipe deflection

$$\frac{dU}{dx} = \frac{P}{A_p E} \tag{7}$$

c. Soil deflection

$$\frac{dU_s}{dr} = \frac{\tau}{G_s} \tag{8}$$

d. Soil force balance

$$2\pi r\tau = -2\pi R_H \tau_H + \pi \gamma_s (R_H^2 - r^2) \tag{9}$$

2.2 Boundary Conditions

The loads on the pipe are due to the initial weight of the pipe, the stemming, and thermal stress effects caused by the temperature difference between the stemming and the pipe. When each layer of stemming is added the pipe deflects into the previous layers. This causes the shear stress at the pipe wall to be reduced and may change sign until it reaches a maximum at which point the pipe slips locally.

As a result, the initial deflection on the pipe when each layer is added depends on the past history. Therefore, the boundary conditions on the soil-pipe interface are nonlinear and mixed, i.e. force and displacement. The boundary conditions on the pipe ends are:

Pipe

$$U = 0 \text{ at } X = 0$$

$$P = 0 \text{ at } X = L_o$$

When the load, P_{max}, is specified at the pipe support we have

$$P = P_{max} \text{ at } X = 0$$

$$P = 0 \quad \text{at } X = L_o$$

The boundary conditions on the soil-pipe interface at any position x are

Soil-Pipe

$$r = R_H \qquad U_s = 0$$

$$r = r_p \qquad U_s = U - U_o$$

where U_o is the deflection of the pipe due to previous stemming and is a nonlinear function of x. When slip occurs $|\tau_p| \geq \tau_{pmax}$

we have

$$r = R_H \qquad U_s = 0$$

$$r = r_p \qquad \tau_p = \text{Sgn}\,(\dot{\tau}_p)\,\tau_{pmax}$$

The solution of Eqs. 1 to 4 are the accompanying nonlinear boundary conditions will be accomplished by the numerical finite element method described in the next section.

3.0 Finite Element Analysis

3.1 Finite Element Model

The stemming process described by Eqs. 6 to 9 and the non-linear boundary description can be conveniently solved by finite element techniques. The method consists of dividing the pipe into n elements and adding soil to each element as the stemming rises in the hole. The initial deflection of the pipe due to previous stemming are initial conditions for each new element.

The stemming region is modeled by slip and no-slip elements with thermal stresses such that the shear stress at the pipe does not exceed the maximum allowable. The region above the stemming is treated by conventional bar elements. The various element stiffness matrices are added together by the direct stiffness method and the loads at the nodes as stemming rises are obtained by the solution of n equations n times. The details are described in the next section.

3.2 Numerical Solution

The numerical procedure is to solve for the nodal loads on the pipe by the direct stiffness method. The matrix representation of the system of n equations and n unknowns is

$$\{P\} = [K]\,\{U\} + \{F\} + P_I \qquad (10)$$

where P is the load vector, K is the merged stiffness matrix, U is the displacement vector, F is the body force vector made up of the shear and thermal stress effects, and P_1 is the initial load given by Eq. 5. The boundary conditions are:

$$U_1 = 0 \text{ at } x = 0$$
$$P_{n+1} = 0 \text{ at } x = L_o \qquad (11)$$

The boundary condition for load release, i.e., the collar load, is designed to carry a load equal to no greater than P_{max} is

$$P_1 = P_{max} \text{ at } x = 0$$
$$P_{n+1} = 0 \text{ at } x = L_o \qquad (12)$$

Boundary conditions (11) are applied until $P = P_{max}$ and then (12) are applied. The loads on the pipe as the stemming rises is obtained by solving Eq. (10) each time a soil element is added until the hole is filled.

3.3 Element Stiffness Matrices

The element matrices which make up the component parts of the global stiffness matrix K in Eq. 10 are:

a. Pipe element (Fig. 5a)

The nodal loads for the pipe element can be derived from Fig. 5a or obtained from Przemieniecki.[8] They are:

$$P_1 = \frac{A_p E}{L} (-U_1 + U_2) \qquad (13)$$

$$P_2 = \frac{A_p E}{L} (-U_1 + U_2) \qquad (14)$$

where P_1 and P_2 are the nodal loads, U_1 and U_2 are the nodal displacements, L is the element length. The stiffness matrix representation of Eqs. (10) and (11) in terms of local coordinates is:

$$\begin{bmatrix} P_1 \\ P_2 \end{bmatrix} = \frac{A_p}{L} \begin{bmatrix} 1 & -1 \\ -1 & 1 \end{bmatrix} \begin{bmatrix} U_1 \\ U_2 \end{bmatrix} \qquad (15)$$

b. Nonslip soil-pipe element (Fig. 5b)

The nodal loads for the nonslip soil-pipe element are derived from Eqs. 6 to 8. Where x is the local coordinate defined in Fig. 5b. Substituting Eq. (9) and (8) we get

$$G_s \frac{dU_s}{dr} = -\frac{R_H \gamma_H}{r} + \frac{\gamma_s R_H^2}{2r} - \frac{\gamma_s r}{2} \qquad (16)$$

The boundary conditions are

$$\begin{aligned} r &= R_H \quad , \quad U_s = 0 \\ r &= R_p \quad , \quad U_s = U - U_o \end{aligned} \qquad (17)$$

where U_o is the deflection of the pipe due to previous stemming and is an unknown function of x.

Integration of Eq. 16 yields:

$$U - U_o = A \gamma_H + B \qquad (18)$$

where $A = \frac{R_H}{G_s} \ln(R_H/R_p)$ (19)

$$B = -\frac{\tau_s}{2}\frac{R_H^2}{G_s}\ln(R_H/R_p) + \frac{\tau_s}{4G_s}(R_H^2 - R_p^2) \qquad (20)$$

Substitution of (18) into (6) we get

$$\frac{dP}{dx} + \tau_s(R_H^2 - R_p^2) - \frac{2\pi R_H}{A}(U - U_o - B) = 0 \qquad (21)$$

Differentiating we get

$$\frac{d^2P}{dx^2} - \frac{2\pi R_H}{A}\left(\frac{dU}{dx} - \frac{dU_o}{dx}\right) = 0 \qquad (22)$$

Substituting (7) into (22) we get

$$\frac{d^2P}{dx^2} - cP = K_o \qquad (23)$$

where $$c = \frac{2\pi R_H}{AA_pE} \qquad (24)$$

and

$$K_o = \frac{-2\pi R_H}{A}\frac{dU_o}{dx} \qquad (25)$$

The function U_o is globally nonlinear but can be approximated by a piecewise linear function over an element. The solution over an element is

$$P = a\ e^{\sqrt{c}x} + b\ e^{-\sqrt{c}x} - \frac{K_o}{c} \qquad (26)$$

A linear approximation for U_o over an element means that a layer of sand of thickness L is instantly applied to the initial displacement distribution U_o of the element shown in Fig. 4a. U_o is given by

$$U_o = U_{o1} + \left(\frac{U_{o2} - U_{o1}}{L} \right) x \qquad (27)$$

where U_{o1} and U_{o2} are the initial displacements at nodes 1 and 2, due to previous stepping, L is the length of an element, x is the local coordinate and

$$F_o = - \frac{2 R_H}{A} \frac{(U_{o2} - U_{o1})}{L} \qquad (28)$$

The boundary condition on the element at x = 0 is

$$\frac{dP}{dx} = - \rho_c (R_H^2 - w_p^2) + \frac{2 R_H}{A} (U_1 - U_{o1} - B) \qquad (29)$$

and x = L

$$\frac{dP}{dx} = - \rho_s (R_H^2 - R_p^2) + \frac{2 R_H}{A} (U_2 - U_{o2} - B) \qquad (30)$$

Differentiating (26) and substituting into (29) and (30) we get

$$a \bar{c} - b \bar{c} = K_1 U_1 + K_2 \qquad (31)$$

$$a \bar{c} e^{\bar{c}L} - b \bar{c} e^{-\bar{c}L} = K_1 U_2 + K_3 \qquad (32)$$

where $K_1 = \frac{2 R_H}{A}$

$$K_2 = - \rho_c (R_H^2 - R_p^2) - \frac{2 R_H}{A} (U_{o1} + B) \qquad (34)$$

$$K_3 = - \rho_s (R_H^2 - R_p^2) - \frac{2 R_H}{A} (U_{o2} + B) \qquad (35)$$

Solving Eqs. (31) and (32) for a and b we get

$$a = \frac{1}{\sqrt{c}} (K_1 U_1 + K_2) + b \tag{36}$$

$$b = \frac{K_1(U_2 - U_1 e^{\sqrt{c}L}) - K_2 e^{\sqrt{c}L} + K_3}{\sqrt{c}\,(e^{\sqrt{c}L} - e^{-\sqrt{c}L})} \tag{37}$$

The nodal forces are

$$P_1 = a + b - K_o/c \qquad \text{at } x = 0 \tag{38}$$

$$P_2 = ae^{\sqrt{c}L} + be^{\sqrt{c}L} - K_o/c \quad \text{at } x = L \tag{39}$$

Substituting for a and b we get

$$\begin{bmatrix} P_1 \\ P_2 \end{bmatrix} = \begin{bmatrix} -\frac{K_1 C_1}{C_2} & \frac{2K_1}{C_2} \\ -\frac{2K_1}{C_2} & \frac{K_1 C_1}{C_2} \end{bmatrix} \begin{bmatrix} U_1 \\ U_2 \end{bmatrix} + \begin{bmatrix} \frac{2K_3 - K_2 C_1}{C_2} - \frac{K_o}{c} \\ \frac{K_3 C_1 - 2K_2}{C_2} - \frac{K_o}{c} \end{bmatrix} \tag{40}$$

where $C_1 = e^{\sqrt{c}L} + e^{-\sqrt{c}L}$ and $C_2 = e^{\sqrt{c}L} - e^{-\sqrt{c}L}$

Transforming the first equation above to local coordinates we obtain the soil pipe stiffness matrix representation

$$\begin{bmatrix} P_1 \\ P_2 \end{bmatrix} = \begin{bmatrix} \frac{K_1 C_1}{C_2} - \frac{2K_3}{C_2} \\ \frac{-2K_1}{C_2} \quad \frac{K_1 C_1}{C_2} \end{bmatrix} \begin{bmatrix} U_1 \\ U_2 \end{bmatrix} + \begin{bmatrix} \frac{K_2 C_1 - 2K_3}{C_2} + \frac{K_o}{c} \\ \frac{K_2 C_1 - 2K_2}{C_2} - \frac{K_o}{c} \end{bmatrix} \tag{41}$$

c. Soil-pipe element with slip (Fig. 5c)

When the shear stress on the pipe τ_p becomes

$$\tau_p = \tau_{pmax} \tag{42}$$

the non-slip element is changed to a slip element. Thus when slip occurs at $r = R_p$

$$\tau_p = \text{sgn}(\tau_p)\ \tau_{pmax} \tag{43}$$

Combining Eqs. (6), (9), and (43) we have

$$\frac{dp}{dx} = 2\pi R_p\ \text{sgn}(\tau_p)\ \tau_{pmax} \tag{44}$$

The stiffness matrix for this equation is similar to the pipe element i.e.

$$\begin{bmatrix} P_1 \\ P_2 \end{bmatrix} = \frac{A_1 E}{L} \begin{bmatrix} 1 & -1 \\ -1 & 1 \end{bmatrix} \begin{bmatrix} U_1 \\ U_2 \end{bmatrix} + \pi R_p\ \text{sgn}(\tau_p)\ \tau_{pmax} \begin{bmatrix} -1 \\ -1 \end{bmatrix} \tag{45}$$

d. Thermal stresses

When the temperature of the stemming material is different than the ambient temperature, thermal stresses are enduced in the pipe. Thermal stresses induced while the stemming is using is accounted for by adding to the soil pipe elements the thermal body force given by

$$\begin{bmatrix} p_1 \\ p_2 \end{bmatrix} = A_p E \alpha \Delta T \begin{bmatrix} 1 \\ -1 \end{bmatrix} \tag{46}$$

where α is the coefficient of thermal expansion and $\Delta T = T - T_0$ is the temperature change. Further information on the deviation of stiffness matrices can be found in Przemieniecki.[8]

4.0 Material Properties

The shear modulus G_s and the coefficient of function μ_p are required input to STMLOD. Their values depend on the average stress in the stemming column which is given by Eq. A8 to be

$$\sigma = \frac{\tau_s}{2K}\left(\frac{R_H^2 - R_p^2}{\mu_H R_H + \mu_p R_p}\right) = 3.26 \text{ psi}$$

where $\mu_p = .6$, $\mu_H = .6$, $K = .6$, $\tau_s = 94$ lb/ft^2, $R_H = 4.0$ ft, and $R_p = .40$ ft. are typical values.

The constant μ_p is used in calculating the maximum allowable shear stress at which pipe slip occurs. When $|\tau_p| = \tau_{pmax}$ we set $\tau_p = \text{sgn}(\tau_p)\tau_{pmax}$. The functional form of τ_{pmax} is derived from Eq. A8 and A10 is given by

$$\tau_{pmax} = \frac{\mu_p \gamma_s}{2}\left(\frac{R_H^2 - R_p^2}{\mu_H R_H + \mu_p R_p}\right)$$

where μ_H is the coefficient of function at the hole wall. Values of μ_p at low stress levels, σ 2 to 3 psi, are estimated from Fig. 22 of Ref. 9. For overton sand we have μ_p .9 to 1. and pea gravel μ_p .45 to .5. Values for LLL-mix, colemanite, and magnitite are assumed to be the same as overton sand. The coefficient of friction at the hole wall for all stemming materials is estimated from Ref. 14, Table 3.3.1 to be μ_H .6 to .95.

The shear modulus G_s is a measure of the stiffness of the stemming material. The stiffer the material the greater the load transfer from the pipe to hole wall, consequently less load on the pipe. Values for G_s are not well known, however, we have available to us the confined stress-strain curve for LLL-mix shown in Fig. 5. The slope of the curve is proportional to the shear modulus.

An analytical expression for the shear modulus can be derived (Ref. 10, p. 106) from the stress-strain relation for confined compression given by

$$\sigma_1 = (\gamma + 2G_s)\, \varepsilon_1$$

where $\lambda = \frac{2\nu G_s}{1-2\nu}$ and ν is Poissons ratio.

The confined Youngs modulus becomes

$$E_s = (\lambda + 2G_s)$$

and the shear modulus becomes

$$G_s = \frac{1-2\nu}{2(1-\nu)}\ E_s = .286\ E_s$$

where $\nu = .3$ is common for most substances.

The results are

σ(psi)	E_s (psi)	G_s(psi)
2	250	75
3	333	95
4	2960	847

The shear modulus is nonlinear over a range of stresses but the stemming column experiences a nearly constant stress of approximately 3.3 psi over most of its length, therefore a local linear approximation is adequate. An average value of G_s = 120 psi for LLL-mix gives the best results when comparing STMLOD calculations with test data.

The value of G_s = 40 psi for overton sand, colemanite, and magnitite are derived from matching STMLOD calculations with data. Pea gravel is stiffer than LLL-mix so a value of G_s = 130 psi was chosen. Since pea gravel slips on the pipe μ_p is more important while G_s can be approximate. Additional

information on formulas for estimating Poissons ratio and Janssen's constant K is given by Blake and Zaslawsky.[9] A summary of the constants used in STMLOD are given in Table 1.

TABLE 1

Material Constants and Stresses for Stemming Materials*

Material	γ_s (lb/ft^3)	Eq.A8 (psi)	Eq.A10 τ_{pmax} (psi)		K	μ_H **	μ_p	G_s (psi)
LLL-mix	94	3.07	1.84	.3	.6	.6	1.	120
Pea Gravel	87	3.09	.83	.3	.6	.6	.45	130
Overton Sand	100	3.26	1.96	.3	.6	.6	1.	40
Magnetite	170	5.55	3.33	.3	.6	.6	1.	40
Colemanite	88	2.87	1.72	.3	.6	.6	1.	40

* The material constants are subjected to change when more experimental data is recieved and more STMLOD calculations are made and compared to field data.

** μ_H is only used in calculating τ_{pmax}. There is a no-slip condition on the hole wall. μ_p and G_s are the only important constants.

5.0 Results

The results presented here are STMLOD calculations compared to test results on problems of interest to emplacement pipe designers. Sample problems include calculating the loads on pipe in layered and unlayered media and determining the thermal stresses induced by stemming materials at different temperatures.

Figure 7 shows a typical unlayered emplacement scheme and Fig. 8 shows a comparison of STMLOD, STEM, and experimental data. The results show that STEM over predicts the load by 46 percent while STMLOD is in agreement with experimental data, consequently, a lighter design and a cost savings. In the unlayered scheme, it was found that LLL-mix can be modeled without slip i.e. $\mu_p > .85$ while the shear modulus can be adjusted to give good results. The smooth loading curve is indicative of no slipping during stemming. $\mu_p = 1$ was chosen to insure no slip.

Figure 9 shows the emplacement configuration for the new layered stemming plan and Fig. 10 shows a comparison of STMLOD with test results. The most interesting feature the layered scheme is that the loads due to stemming are much lower than their unlayered scheme. This can be accounted for by pipe slippage in pea gravel. The irregularities in the loading curve, Fig.10, are due to pipe slip. In this scheme, it was found that G_s for pea gravel was not to important, i.e. $G_s > 120$ while $\mu_p \approx .45$ was required to produce slip. On the other hand, Quigg [12] has shown that the shear stiffness can be increased to a large number to get results which compare to experiment. Similar calculations were done on STMLOD but G_s had to be made so large that it is physically unrealistic. The deflections of the pipe, however, are not correct.

Figure 11 shows the emplacement configuration for a layered design where thermal stresses are important. Figure 12 shows a comparison of the temperature distribution and approximations used in STMLOD calculations. Figure 13 shows the results of STMLOD with and without thermal stresses as compared to test data with thermal stress. The results show that thermal stress induced by hot materials during stemming reduce the loads. However, when the stemming cools the loads should increase. A better calculations can be made by refining the grid so the temperature distribution shown in Fig. 12 can be more closely approximated.

6.0 Summary and Conclusions

The new formulation has reduced the six constants to two measurable material constants. Load release due to support subsidence can be calculated. Excellent agreement with experiment has been obtained for layered and unlayered stemming schemes. Pipe slip and thermal stresses have been accounted for. Concentrated loads on the pipe are easily added. The effect of adding mud in the pipe at any time can be calculated. The new code will reduce the conservatism of the old STEM code and thus realize a cost savings. Furthermore, the formalism is based on refined mechanics and fundamental material constants. It will provide greater confidence and flexibility in design. Finally, the STMLOD code is six times faster than the STEM code.

7.0 Acknowledgements

I would like to thank the diagnostic engineers of the Nuclear Test Engineering Division for reviewing the manuscript and supplying STEM calculations, drawings, and test data.

8.0 References

1. Hamilton, W. A., "Stemming Loads on Emplacement Systems," LRL Planning and Construction Report, ANS 9-3288, (August 1969).
2. Norris, D. M., "Stemming Loads - A Mathematical Model", ENN 70-48, (July 1970).
3. Norris, D., Jr., J. Staats, and W. Kleck, "STEM - A Computer Program for Calculations of Stemming Loads," UCID-30049 (June 1972).
4. Staats, J. R., "The STEM Program - Status and Potential," ENN 73-105, (May 1973).
5. Blake, A., "STEM Code - A Correlation of Theory and Experiment," ENN 75-37 (March 1975).
6. Maiden, D. E., "User's Manual for STMLOD - A Computer Program for Calculating the Stemming Loads on the Pipe String," ENN 77-62 (1977).
7. Taylor, A., private communication. (September 1976).
8. Przemieniecki, J. S., "Theory of Matrix Structural Analysis," McGraw-Hill, 1968.
9. Blake, A. and M. Zaslawsky, "Behavior of Stemming Materials Under Stress," UCRL-51034 (April 15, 1971).
10. Jaeger, J. C. and N. G. W. Cook, "Fundamentals of Rock Mechanics," Chipman and Hall LTD (1969), p. 88.
11. Janssen, H. A., "Versuche uber Gelrudedrud in Solozellen," Zeit. Ver. deut. Ingr. 39, 1045 (1895).
12. Quigg, J. D., "Determination of a Suitable Value of Pea Gravel Soil Stiffness for Use with the STEM Code," ENN 79-9, Feb. 15, 1979.

9.0 Appendix

The variation of vertical stress σ is small, therefore, the $\frac{d\sigma}{dx}$ terms in equations 1 and 3 can be neglected. This can be seen from the solution for the stress distribution when the pipe is rigid. Given Coulomb's failure criteria

$$\tau = \mu \sigma_{HOR} + C \qquad A1$$

where τ is the shear stress, μ the coefficient of friction, σ_{HOR} is for our use the horizontal stress, and C the cohesion. We also have Janssen's formula[11] relating the horizontal stress to the vertical stress

$$\sigma_{HOR} = K\sigma \qquad A2$$

where K is Janssen's constant and σ is the vertical stress. Combining equations A1 and A2 we have at the hole wall

$$\tau_H = \mu_H K\sigma + C_H \qquad A3$$

and at the pipe wall

$$\tau_p = \mu_p K\sigma + C_p \qquad A4$$

Substituting Eqs. A1 and A4 into Eq. 3 and assuming the cohesions $C_H = 0$ and $C_p = 0$ we have

$$\frac{d\sigma}{dx} + \lambda\sigma = \gamma_s \qquad A5$$

where

$$\lambda = \frac{2K(\mu_H R_H + \mu_p R_p)}{R_H^2 - R_p^2} \qquad A6$$

The solution is

$$\sigma = \frac{\gamma_s}{\lambda} [1 - \exp(-\lambda x)] \tag{A7}$$

For $x > 2.5R_H$ the vertical stress approaches the asymptotic value

$$\sigma = \frac{\gamma_s}{\lambda} = \frac{\gamma_s}{2K} \left(\frac{R_H^2 - R_p^2}{\mu_H R_H + \mu_p R_p} \right) \tag{A8}$$

The shear stress at the hole wall becomes

$$\tau_H = \mu_H K \sigma \tag{A9}$$

and at the pipe wall

$$\tau_p = \mu_p K \sigma \tag{A10}$$

If $\mu_H = \mu_p$ we have the "wetted parimeter" shear stress

$$\tau_H = \tau_p = \frac{\gamma_s}{2} (R_H - R_p) \tag{A11}$$

Equation (A11) can also be arrived at by taking the ratio of the weight of the annulus $\gamma_s \pi (R_H^2 - R_p^2) L$ divided by the total perimeter $2 \pi (R_H + R_p)$. The load on the pipe becomes

$$P = 2 \pi \gamma_s (R_H - R_p) R_p (L_o - x) \tag{A12}$$

This is called the "wetted perimeter load".

The rigid pipe solution, Eq. A7, shows that the axial stress approaches a constant value when $x \cdot 2.5\ R_H$ and the length of the $L_o \cdot\cdot R_H$. Similarly the effect of the elasticity of the pipe should have a small perturbation on the variation of the axial stress field. Therefore $\frac{d}{dx} \approx 0$ is a good approximation. Moreover, the inaccuracy in modeling the stemming process and the material properties do not warrent further refinement. Finally, the true test is that the model gives acceptable results within engineering accuracy.

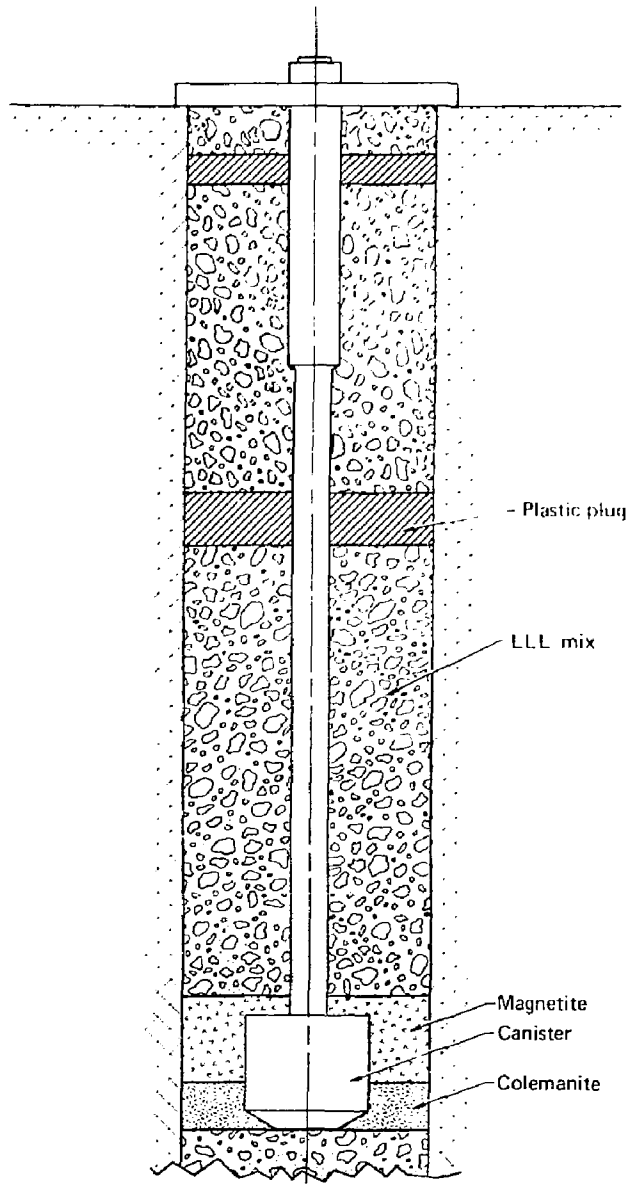

Figure 1. Unlayered LLL-mix stemming scheme.

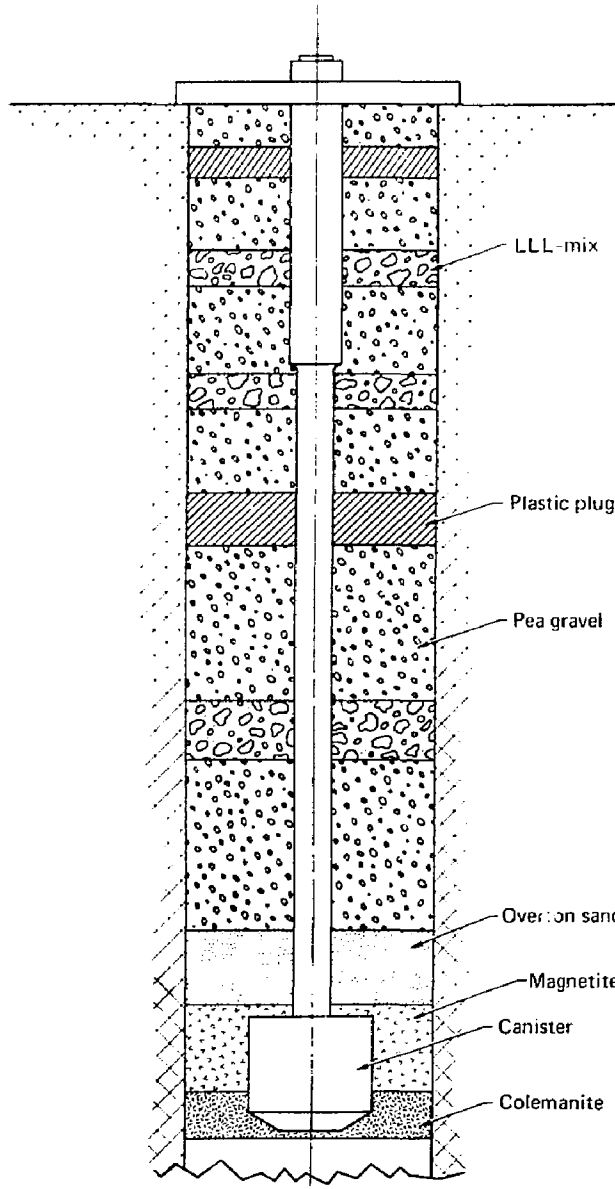

Figure 2. Layered LLL-mix, pea gravel stemming scheme.

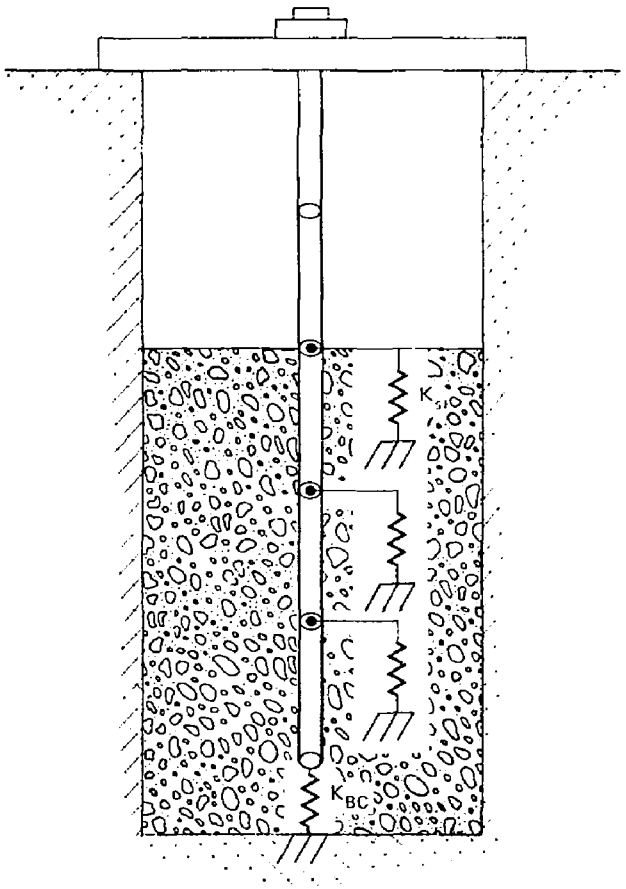

Figure 3. Computational model for the STEM code showing the soil support springs Ks.

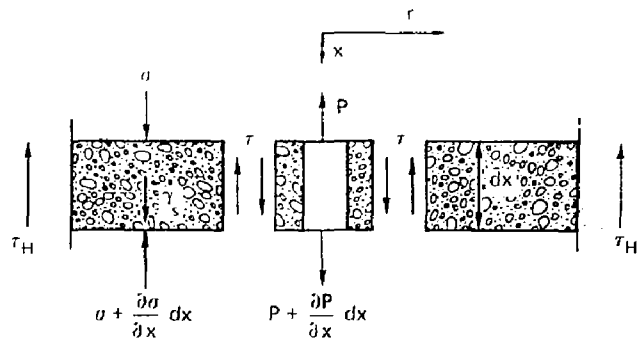

Figure 4. Free body diagram for the soil and pipe.

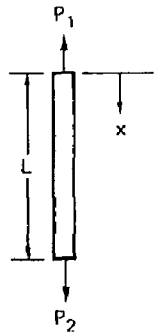

a. Pipe element

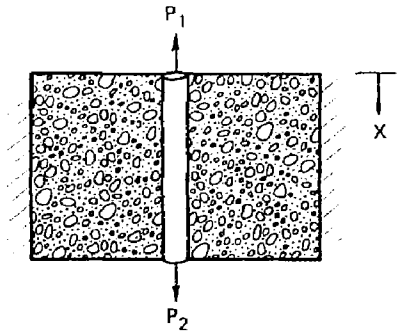

b. Nonslip soil-pipe element

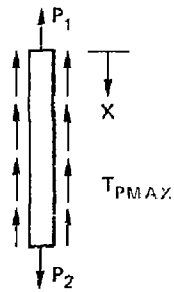

c. Soil-pipe element with slip

Figure 5. Finite element models.

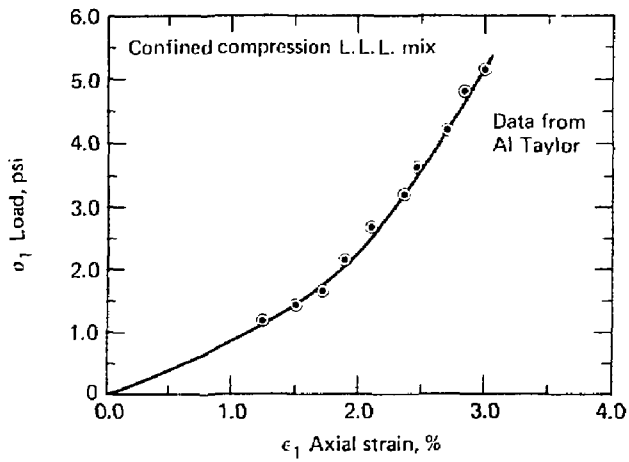

Figure 6. Confined compression test for LLL-mix taken by Al Taylor[7].

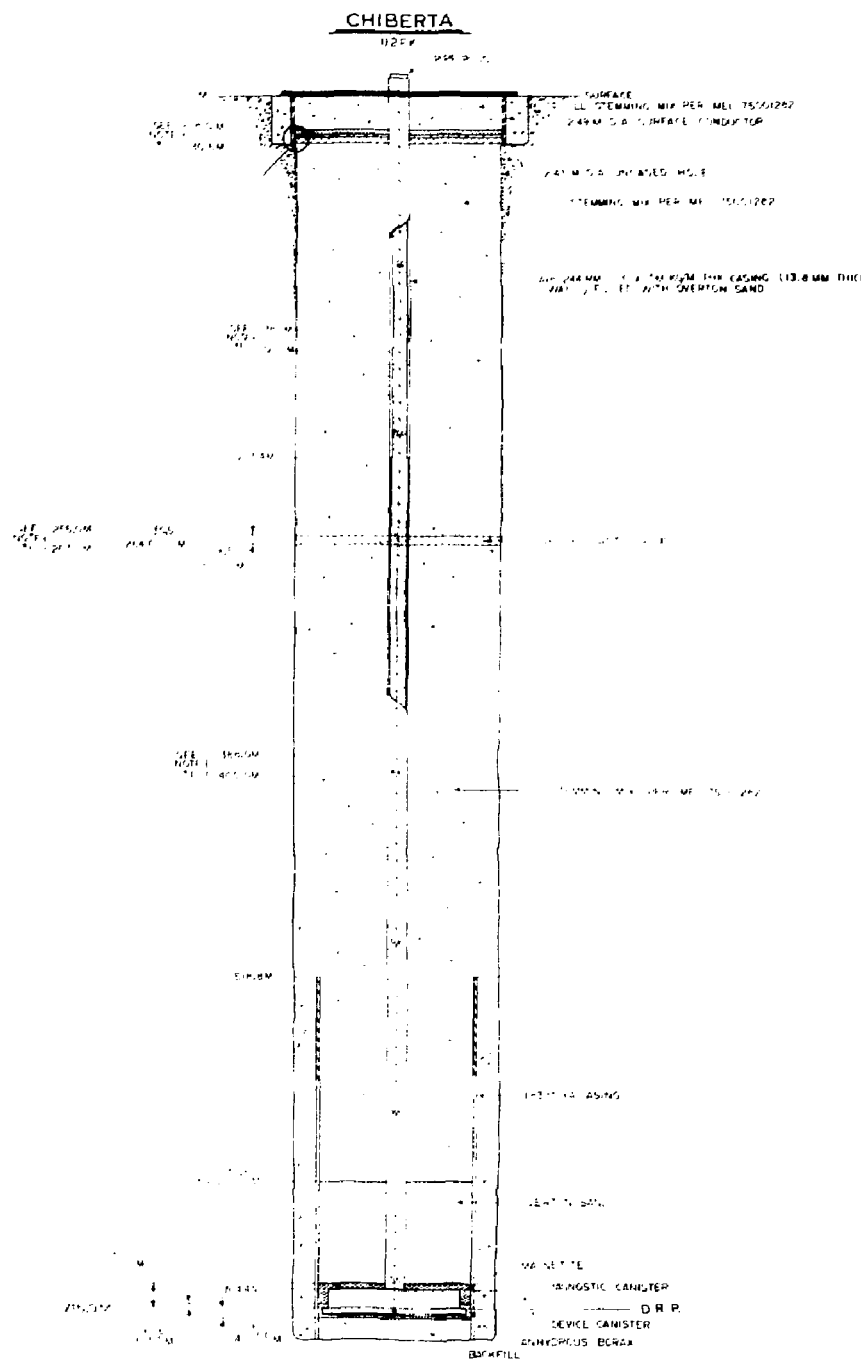

Figure 7. Pipe implacement configuration for CHIBERTA.

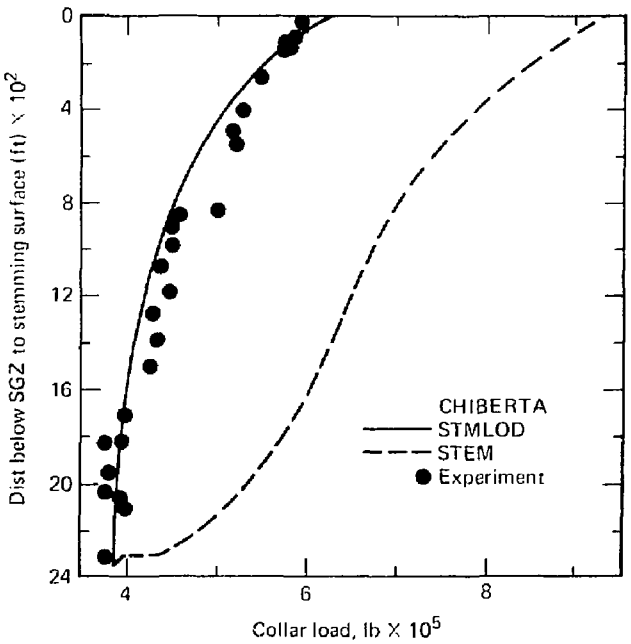

Figure 8. Comparison STMLOD, STEM, and test for CHIBERTA.

EMMENTHAL

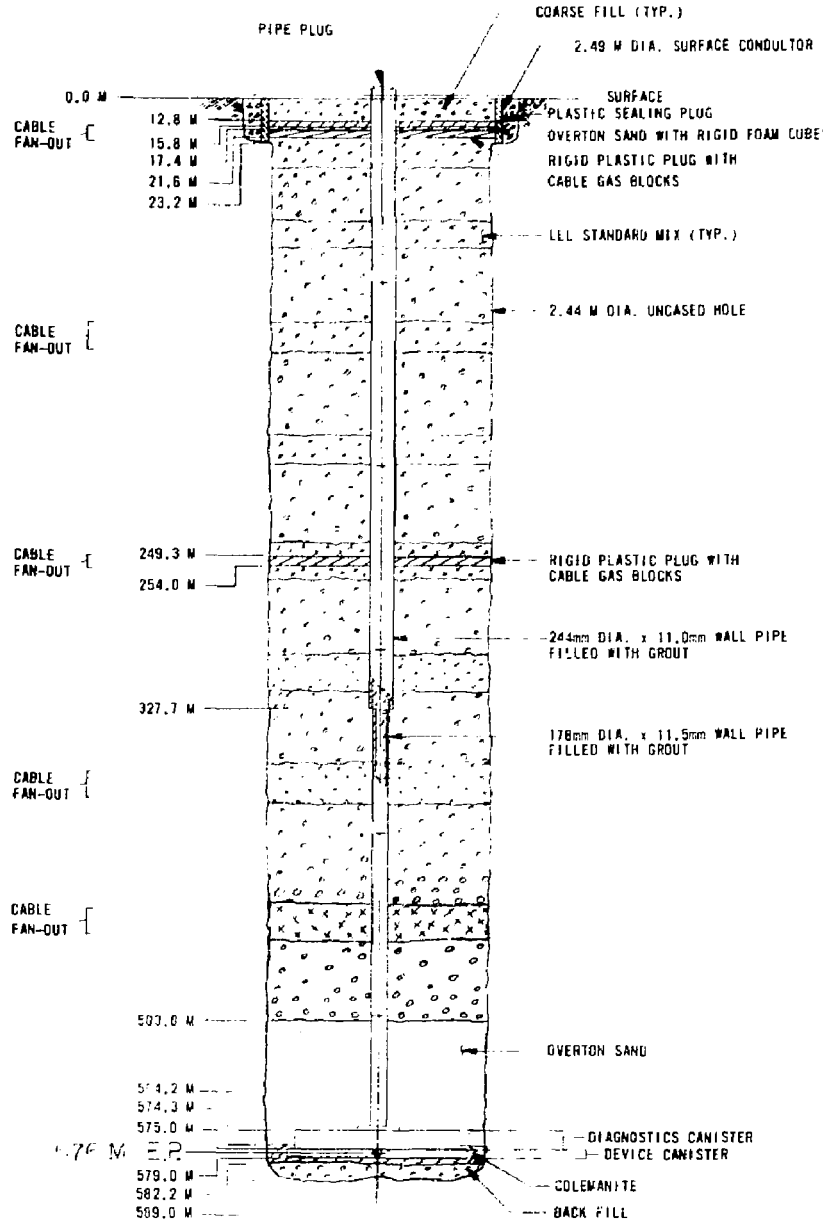

Figure 9. Pipe implacement configuration for EMMENTAL.

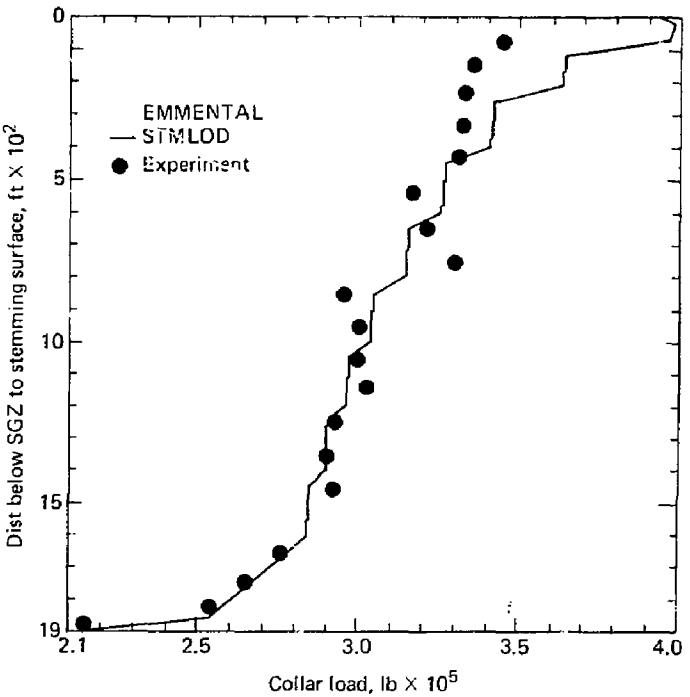

Figure 10. Comparison of STMLOD and test for EMMENTAL.

KLOSTER

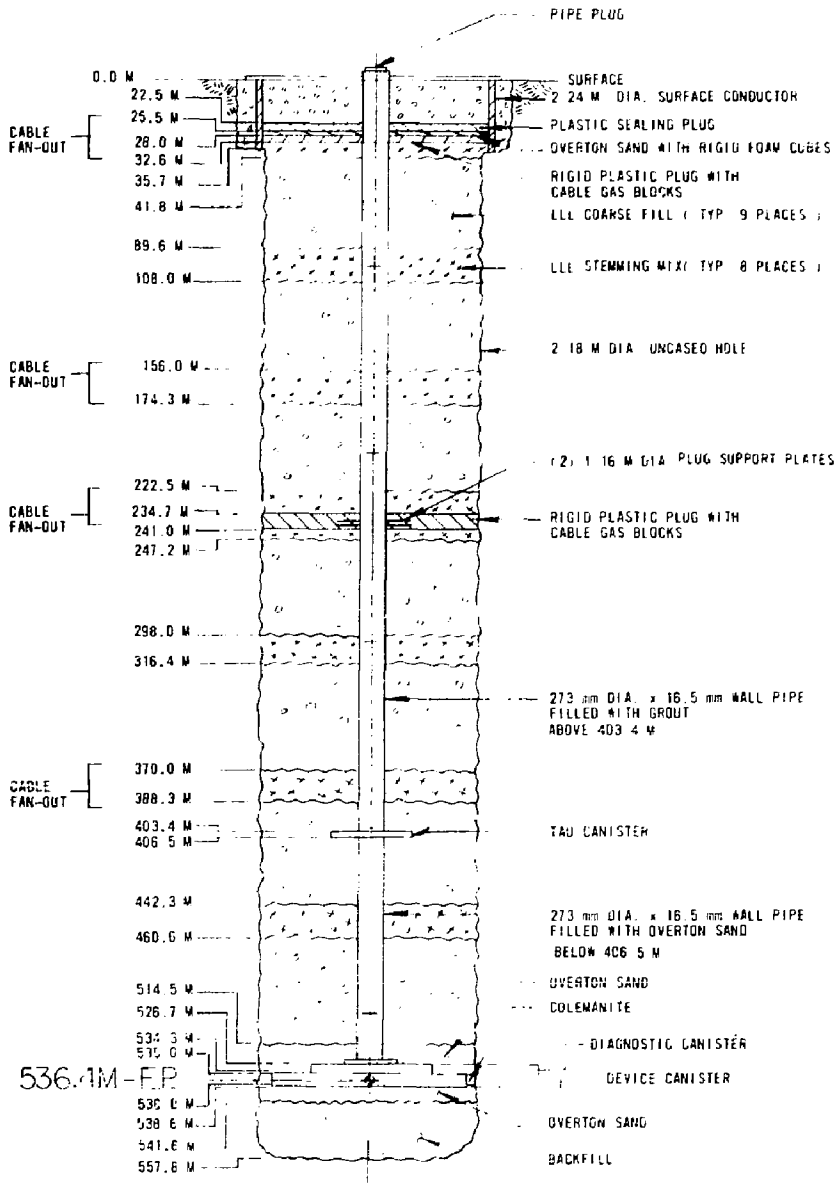

Figure 11. Pipe implacement configuration for KLOSTER.

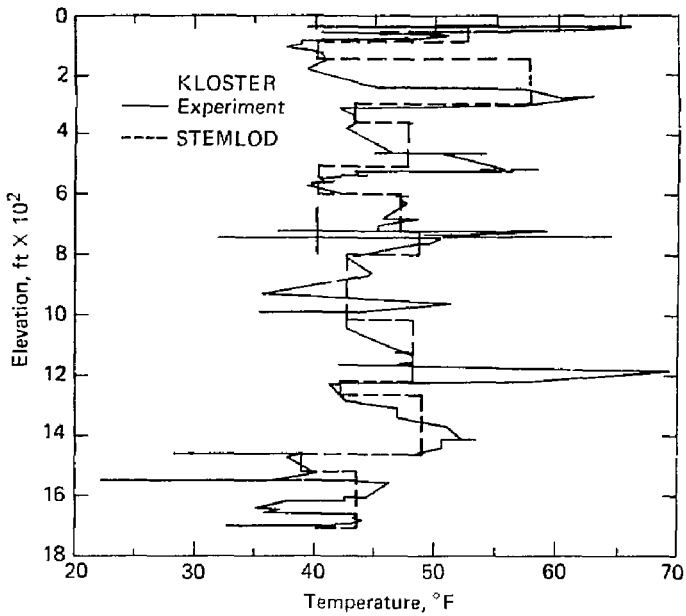

Figure 12. Comparison of the temperaturedistribution as stemming rises with that used for STMLOD calculation of KLOSTER.

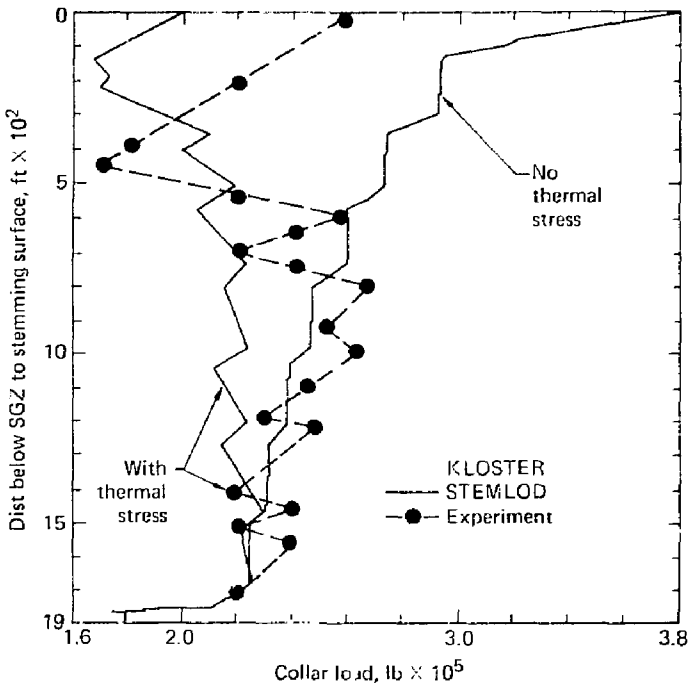

Figure 13. Comparison of STMLOD, and test for KLOSTER.